Efficient shear retrofitting of reinforced concrete beams using prestressed deep embedded bars

Bhanugoban, Maheshwaran; Yapa, Hiran; Dirar, Samir

DOI:
10.1016/j.engstruct.2021.113053

Efficient Shear Retrofitting of Reinforced Concrete Beams using Prestressed Deep Embedded Bars

Maheshwaran Bhanugoban[1], Hiran Yapa[1*], Samir Dirar[2]

[1]University of Peradeniya, Sri Lanka

[2]University of Birmingham, UK

[*]Corresponding author

Civil Engineering Department

Engineering Faculty

University of Peradeniya

Peradeniya, 20400

Sri Lanka

hdy@pdn.ac.lk

Abstract

The Deep Embedment (DE) technique is a promising reinforced concrete (RC) shear strengthening scheme. When compared with the other retrofitting systems, the DE approach is impressive in many ways. Particularly, since the DE element is installed to the beam core, the truss mechanism is enhanced and that enables achieving high shear enhancements. Due to the internal application of the DE reinforcement, steel can also be utilized as the retrofitting material without reservations on corrosion. It is however identified that the tensile capacity of the DE bar is partially utilized. In this context, the potential of using prestress in the DE system as an improvement was explored through a non-linear numerical study and an experimental study. Two DE reinforcement types of normal steel and high-tensile steel were considered and the prestress level was set to 40%. Both approaches showed that the use of prestress in the DE system was capable of enhancing the beam shear capacity significantly, and the extra shear strength gain in one beam was almost 26%. The serviceability performance of the beams was also improved due to the prestress application. Meanwhile, the numerical predictions showed good correlations with the global and local behaviours of the experimental beams.

Keywords: Deep embedment; non-linear modelling; prestress; reinforced concrete; shear retrofitting

1. Introduction

Shear strength deficiencies in reinforced concrete (RC) structures arise due to numerous reasons including increased loadings, changes in use, material deterioration, and poor detailing [1-3]. Since RC shear failure is inherently brittle and catastrophic, serious attention to shear-deficient RC structures is utterly important. From an engineering perspective, when compared with the general remedial actions of imposing load limits and demolishing-and-reconstruction, structural retrofitting is an appealing solution [3,4]. The major merits of retrofitting include less interruption to users, enhanced sustainability credentials, and better utilisation of resources. However, given that shear behaviour of concrete is not fully understood, design and implementation of shear retrofitting systems have to be carried out extremely carefully [5-7].

Shear retrofitting of RC structures evolved from external application of reinforcement to the shear span of a structure. The use of fibre reinforced polymer (FRP) materials as retrofitting elements has been popular because of their non-corrosive nature which is ideal for external usage. The externally bonded (EB) technique was the pioneering FRP shear retrofitting system. In this method, the retrofitting material is bonded along the shear span of a RC member. The effectiveness of the EB FRP shear strengthening technique is well documented [7-9], however, premature de-bonding of the unanchored retrofitting material is an inherent drawback [10-12]. As an improvement, the near-surface mounted (NSM) technique was developed where the retrofitting elements are installed in groves that are cut into the surface [13]. In contrast to the EB system, the NSM technique provided a higher strengthening efficiency [13,14], however, de-bonding remained an issue that prevented optimum use of the system. Meanwhile, Lees et al. [1] developed an unbonded, prestressed Carbon FRP (CFRP) strap shear retrofitting system which eliminates the de-bonding issue. The strap system achieved high levels of shear enhancement, mainly due to the effective use of the high strength in the CFRP straps via the application of prestress [15,16]. However, the strap system is difficult to install and is susceptible to damage during service.

The deep embedment (DE) technique (also called the embedded through-section (ETS) method) can be identified as a relatively novel shear strengthening method [17]. This approach was developed by Valerio and Ibell [5] and can be distinguished from the previously mentioned systems, because the retrofitting element is installed into the core of the RC member. Since the retrofitting element is internal and protected, steel can also be utilised in the system without concerns about corrosion, and it was proved that steel and FRP reinforcement provide comparable shear strength enhancement [5]. In the DE method, vertical or inclined holes are drilled into the concrete upwards from the soffit. High viscosity epoxy resin is injected and FRP or steel bars are subsequently embedded, see **Fig. 1**. The main advantage of the DE system is that the retrofitting bars tie the top chord to the bottom chord of the beam in such a way that the truss action within the beam is enhanced [18]. Moreover, the DE method relies on the concrete core to transfer stresses between the concrete and the FRP/steel; a better bond performance therefore ensues due to confinement [5,14]. Shear enhancement levels of almost up to 100% were achieved in the experiments conducted by Valerio et al. [6], thereby verifying the efficacy of the system. The DE method is ideal for structures where only the soffit of the structure is accessible. Protection against fire and vandalism, less epoxy consumption, and savings on time required for surface preparation of the beam are added merits [5,19].

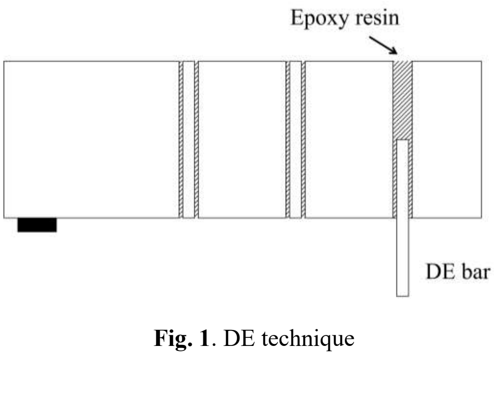

Fig. 1. DE technique

The literature reveals that numerous experimental and numerical studies have been conducted on the DE system. The numerical study by Qapo et al. [20] demonstrated that more accurate results than analytical model (e.g., TR55 [21]) predictions can be obtained from non-linear numerical simulations where the average offset in the numerical prediction was below 8%. It was further identified that concrete strength, a/d ratio and beam depth were governing parameters for the DE system behaviour [17,20]. Also, the interaction between the internal and retrofitting shear reinforcement, hence the relative locations between the two reinforcement types, was identified to be a significant parameter [17,22-24]. Mofidi et al. [22], Breveglieri et al. [23], and Sogut et al. [24] showed that the DE contribution to the shear strength decreases with the increase of the existing shear reinforcement ratio. Meanwhile, Dirar and Theofanous [25] investigated the influence of the shear span-to-effective depth (a/d) ratio on the DE performance and showed that when a/d reduced from 3.0 to 1.9, the shear strength enhancement reduced drastically from 96% to 33%. The bar orientation was also found to be a significant parameter where DE bars inclined at 45˚ were more effective than vertical DE bars [19,23]. Raicic et al. [18] verified the applicability of the DE technique to continuous RC beams. Valerio et al. [6] explored the bond between steel/FRP and concrete using three popular epoxy types and showed that ample bond strength developed in the DE system [6]. Valerio et al. [6] and Chaallal et al. [10] reported that the bond in the DE system was far superior to that in the EB and NSM systems. Mofidi et al. [22] investigated the effect of surface coating on the FRP bars and showed that plain CFRP bars provided higher strength enhancement than sand-coated bars.

Amid many advantages associated with the DE shear retrofitting system, one major drawback is the difficulty of fully utilising the strength of the retrofitting element, particularly for high strength materials [26,14]. Yapa et al. [26] showed that the retrofitted beams failed while considerable capacity remained in the DE element because of the need of fulfilling strain compatibly between concrete, internal steel and the DE elements. Accordingly, the retrofitting efficiency could further reduce if the internal shear reinforcement is in low tensile capacity, e.g., mild steel [26]. The evidence from the behaviour of the CFRP strap system hints that the application of prestress to the DE element could be a potential solution to enhance its performance [2,15,16,27]. It is also possible to show theoretically (e.g., from Mohr's circle) that introducing vertical compressive stress would enhance the shear strength of concrete elements. In this context, this research explores the efficacy of such use of prestress in the DE system through non-linear numerical simulations and an experimental investigation. The scope of the study was limited to the use of steel DE elements.

2. Research significance

The DE technique for concrete shear strengthening has been demonstrated to be an improvement upon other concrete shear strengthening methods. Yet, to date, the vast majority of research studies have focused on the use of passive (i.e., un-prestressed) DE bars. Research on shear retrofitting of RC beams using prestressed DE bars is practically non-existent. This paper presents the first comprehensive numerical and experimental study on RC beams retrofitted in shear using prestressed DE steel bars. The combination of experiments and numerical techniques provided valuable insight into the strengthened behaviour. Besides, the paper identifies the effect of prestress level, DE bar size, and DE bar location on the load carrying capacity of the strengthened beams.

3. Numerical simulation of prestressed DE behaviour

With the primary objective of identifying the effectiveness of using prestress in the DE system, three-dimensional (3D) non-linear finite element simulations were carried out using Midas FEA software package [28]. Considering the fact that most existing RC structures are with mild steel shear reinforcement and, as previously discussed, that scenario represents the least efficient use of DE element strength, RC beams that carry mild steel shear links were considered. Two DE bar types were deployed and those were: (a) normal steel reinforcement bars ($f_{yk} = 500$ MPa); and (b) high-tensile steel bars. Accordingly, the FE modelling included a control beam (notation B1-C), a beam with non-prestressed normal strength steel DE bars (notation B2-NS), a beam with normal steel DE bars with 40% prestress (notation B3-NS-P), a beam with non-prestressed high-tensile steel DE bars (notation B4-HS), a beam with high-tensile steel DE bars with 40% prestress (notation B5-HS-P). In order to highlight the merits of the using prestress, the DE configurations were selected so that to provide nominal strength augmentation. It is of note that the second label in the beam notation indicates whether the normal steel (NS) or high-tensile steel (HS) were used as DE elements and the third notation indicate if the DE bars were prestressed or not.

3.1. Beam model detailing

The geometry for the beam specimens were adopted from previous studies [15,26], where the dimensions were: 1750 mm length; 280 mm depth; and 105 mm width. The beams were subjected to three-point bending loading where the shear span was 690 mm and the pertaining shear span to effective depth ratio (a/d) was close to three. The beam was provided with high level of flexural reinforcement and low level of shear reinforcement to promote shear failure and to have a large gap between the shear and flexure capacities. The internal reinforcement detailing was: 4 H12 bars as compression reinforcements; 4 H16 bars as tensile reinforcements;

and 6 mm mild steel shear links at 200 mm spacing, see **Fig. 2**. For the retrofitting using normal strength steel, two H10 bars were used as vertical DE reinforcements in each shear span. Three 5 mm high strength steel bars were used as vertical DE reinforcements in the other scenario. With the objective of maintaining similarity across the two reinforcement type usage, the number of 5 mm bars was increased to three to balance the force capacity of two H10 bars. The DE reinforcement locations were selected to be the middle region of the internal shear links to minimize interactions between the two types of bars. Accordingly, for B2-NS and B3-NS-P, the DE bar locations were 150 mm and 350 mm measured from the loading point. For B4-HS and B5-HS-P, the DE bar locations were 150 mm, 350 mm, and 550 mm from the loading point, see **Fig. 2**.

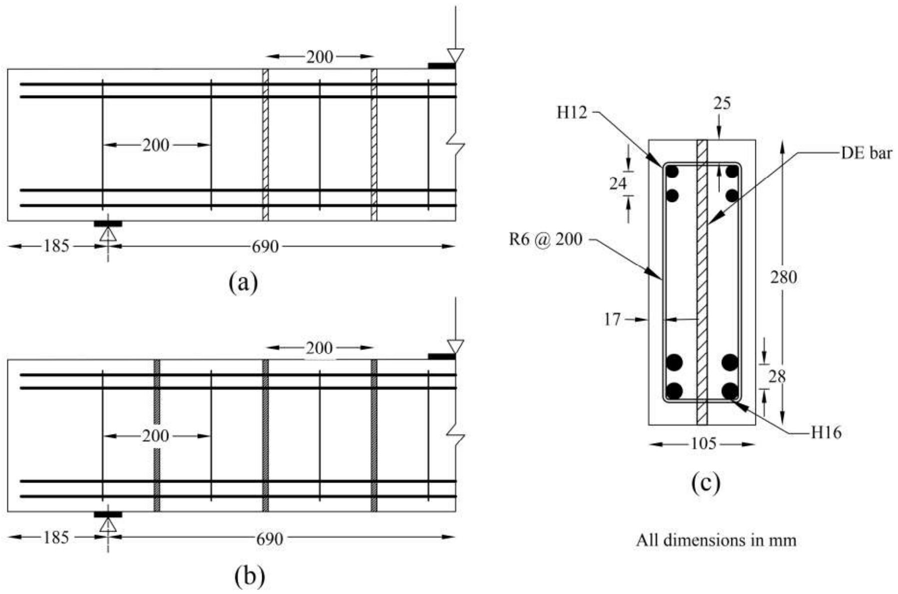

Fig. 2: Beam details; a): elevations of B2-NS and B3-NS-P; b): elevations of B4-HS and B5-HS-P; c): cross section

3.2. Meshing and boundary conditions

Concrete was meshed using eight-node solid brick elements and the bearing plates were meshed with six-node solid wedge like elements. These solid elements consisted of three degrees of freedom per each node. The mesh size was selected to be 25 mm. That particular choice was made presuming the maximum aggregate size to be 12.5 mm and considering the recommendations in [20] that a mesh size of 2-3 times of the maximum aggregate size is appropriate for RC modelling. Meanwhile, the internal longitudinal reinforcements and shear links were meshed with embedded (fully-bonded) reinforcement elements. For modelling of DE steel reinforcements, two-node 3D truss elements supplemented with a bond model were used. To represent the interface between the concrete and the DE steel reinforcements, line embedded interface elements were created along the length of the DE reinforcement. These interface elements ensured the nodal connectivity between the surrounding concrete elements and the DE reinforcement elements, and they were also capable of adopting the bond-slip material model and of simulating the slip between the concrete and the DE reinforcement.

Considering symmetry, half beam model was developed. To simulate the boundary conditions for 3-point bending, the vertical degree of freedom of the support bearing was restrained whilst the horizontal degree of freedom was restrained at the symmetric boundary. **Fig. 3** depicts the processed meshes.

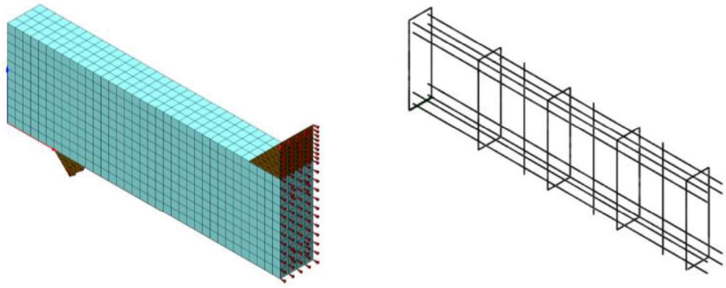

(a) (b)

Fig 3: FE mesh; a) concrete and bearing plates; b) reinforcement

3.3. Material modelling

3.3.1. Concrete

The non-linear cracked behaviour of concrete was simulated with the total strain crack model available in the software. It is a smeared crack-based model and treats the strain in the concrete as a combination of normal strain and crack strain [29]. Either rotating crack or fixed crack options can be assigned to the total strain crack model. The literature provides ample evidence that the shear capacity prediction accuracy achieved from the former is better particularly for RC structures those are with shear reinforcement whereas the latter usually provides over estimations [12,20,30]. Hence, the rotating crack model was opted for the current numerical analysis.

Based on the recommendations found in the literature, the Thorenfeldt relationship for compression and a linear exponential softening curve for tension were identified as appropriate constitutive material models for concrete [4,20]. Accordingly, a target cubic strength of 60 MPa and a target concrete tensile strength of 3.5 MPa were deployed for these functions respectively.

No shear model was adopted. Because the principal stress direction coincides with the crack direction in the rotating crack model, and consequently, there is no shear along the crack. The lateral crack effect [31] and the confinement effect [32] were also incorporated into the simulations. Concrete fracture energy (G_f) was calculated based on the findings of [20], so that: $G_f = 43.2 + 1.13 f_{cu}$. Here concrete cube strength (f_{cu}) is input in MPa and the resultant G_f is in N/m units. Furthermore, the crack band width (h) was assigned to be the cube root of the mesh dimension [29,33]. Concrete stiffness and Poisson's ratio were presumed to be 35 GPa and 0.2 respectively.

3.3.2. Steel

All the target reinforcement bar types were subjected to tensile testing and the stress/strain profiles were established; **Table 1** summarises the results. Based on these findings, a strain hardening function was assigned in the numerical model to simulate the post-yield behaviour of steel and the von Mises criterion available in the software was assigned as the failure criterion.

Table 1

Tensile test results

Reinforcement	Bar type	Yield strength (MPa)	Ultimate strength (MPa)
Tension	H16	504	604
Compression	H12	484	565
Shear	R6	222	342
DE/normal steel	H10	507	597
DE/high-tensile steel	5 mm	*1630	1790

*proof stress

3.3.3. Concrete-DE reinforcement interface

The BPE bond slip model proposed by Eligehausen et al. [34] for embedded steel bars was used to simulate the interfacial behaviour between the concrete and the DE reinforcements. This model comprised an exponential ascending branch followed by a plateau region and then by a linear descending branch as shown in **Fig. 4** (for f_{cu} = 60 MPa and for 10 mm bar)**.** The particular bond model was reported to be successful in predicting the experimental behaviour for various bond conditions [34,35]. Meanwhile, **Fig. 4** also compares the BPE model with the proposals of CEB-FIP Model code 2010 [36] and the comparison shows that the BPE model represents an average scenario for the strong and other bond conditions specified in CEB-FIP Model code 2010.

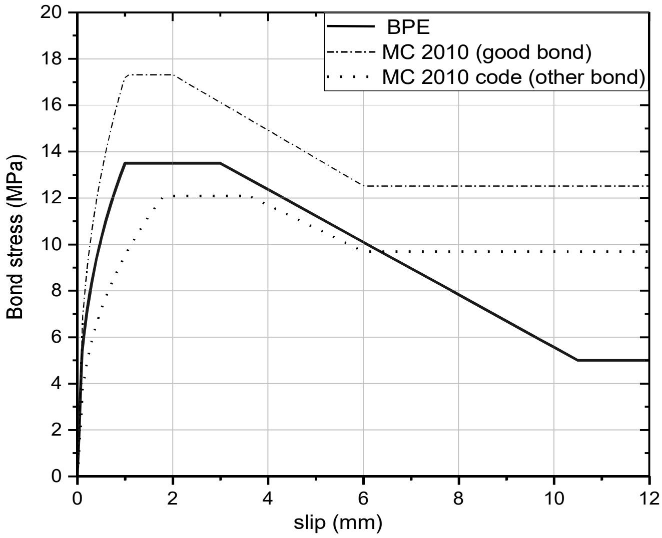

Fig. 4: BPE bond-slip function

3.3.4. Bearing plates

The bearings at the supports and the load point were modelled as perfectly elastic material. Those were assigned with a relatively lower stiffness (of 10 GPa) to facilitate flexibility at the concrete/bearing interface and that was useful to eliminate stress concentrations around the bearings.

3.4 Prestressing of DE bars

The prestress application was simulated using the prestress load option available in Midas FEA. The construction stage analysis option was utilised to separate the prestress loading application and the beam loading application.

The initial prestress level was adopted based on the strain capacity gap between the internal shear links and the normal steel DE bars. Theoretically the strain gap was 50%, and accordingly, together with some residual allowance, 40% prestress was deemed appropriate for the DE bars. A similar level of prestress was applied to the high-tensile DE bars as well.

3.5. Numerical model predictions

The non-linear numerical model predicted all the beams to fail in shear. Considerable shear enhancements were achieved in the retrofitted beams and the application of prestress to the DE bars was highlighted to be effective.

3.5.1 Shear capacity

Table 2 summarises the failure shear loads of the beams. It is observed that the retrofitting resulted in enhancing the shear capacity by 20.3% for B2-NS and by 20.0% for B4-HS specimen. Interestingly, the application of 40% prestress to the DE steel elements has been able to alter the shear enhancement by 10.7% and 6.3% for the normal steel scenario and high-tensile steel scenarios respectively. It will be shown later in the paper that the true effectiveness of the prestress usage towards failure load is even higher than this. It is meanwhile of note that, if perfect bond condition was assigned for the DE bars, the failure load predictions for beams B2-B5 are 101.6 kN, 110.3 kN, 101.6 kN, and 106.3 kN respectively. These values are observed to be fairly equivalent to the pertaining failure loads in Table 2, and hence, as reported in the literature, the bond condition at the DE/concrete interface has been excellent.

Table 2

Shear capacity predictions

Specimen	Failure mode	Shear capacity (kN)	Shear enhancement (%)
B1-C	Shear	83.6	-
B2-NS	Shear	100.6	20.3
B3-NS-P	Shear	109.5	31.0
B4-HS	Shear	100.3	20.0
B5-HS-P	Shear	105.6	26.3

3.5.2 Load-deflection behaviour

The load-deflection behaviour predicted by the FE models for the five beam specimens are illustrated in **Fig. 5**. As should be expected, it shows that all five beams behave similarly at low load levels irrespective of retrofitting differences. Subsequent to the onset of shear cracking, the behaviours become non-linear and the stiffness deteriorates. However, it is interesting to note that the beams with the prestressed DE elements exhibit a stiffer non-linear behaviour in contrast to the other three beams. It is therefore deemed that, in addition to the load capacity increase, the utilisation of prestress in the DE system is also responsible for enhancing the serviceability performance of the beams.

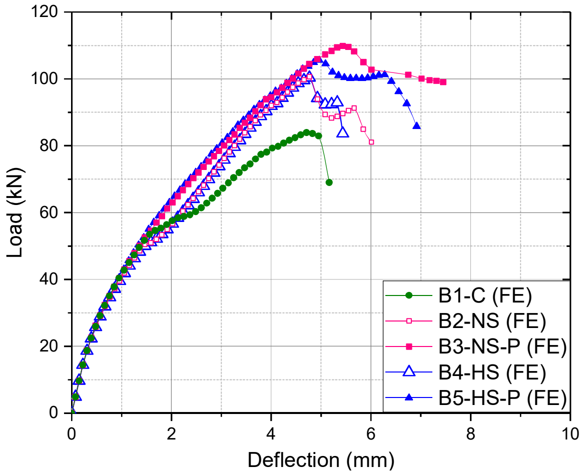

Fig 5. Load - deflection behaviour

3.5.3 Reinforcement strain analysis

To explore the DE bar contribution towards the shear capacity, the strains were analysed. **Fig. 6(a)** compares DE bar strain at its mid-height for non-prestressed and prestressed scenarios of the normal steel usage whilst **Fig. 6(b)** does the same comparison for the high-tensile steel scenario. Note that the locations are illustrated within the plots. As expected, it is highlighted that the application of prestress has been able to utilise more strength from the DE elements. It is observed that the average strain level of the DE element improves due to the application of prestress from 29% to 74% at the normal steel usage and from 10% to 45% at the high-tensile steel usage. Meanwhile, both plots indicate that the critical DE element is always the bar close to the load point whilst the DE3 element (in B4 and B5) that was close the support is almost inactive. That gives an information about the beam area that has to be focused for strengthening, and interestingly, the observation agrees with the moment-shear interactions appreciated in the MCFT theory [37].

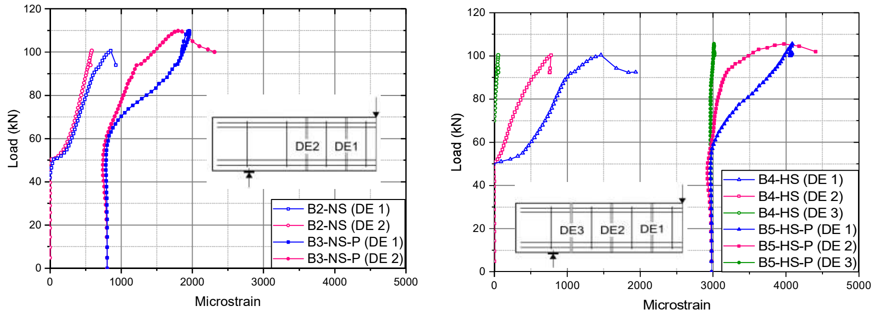

(a) (b)

Fig. 6. DE bar strain; (a) B2-NS vs B3-NS-P; (b) B4-HS vs B5-HS-P

Fig. 7 compares the strain behaviour of internal shear links for the retrofitted beams. When the non-prestressed and prestressed contexts are compared for the beams with normal steel and high-tensile DE steel, the plots clearly indicate that the prestressing has been responsible for reducing straining of the internal shear links. Since, internal links are the critical elements for failure of the beams, such strain control (in the prestressed beams) should have helped the beams to achieve the extra shear enhancements. Interestingly, all the comparisons in **Fig. 7** show that the second shear link from the load point (SL2) is the critical element whereas **Fig. 6** indicated the first DE element from the load point as the critical DE element. It is of note that the first shear link in these beams is almost underneath the load point and hence is subjected to high level of lateral pressure confinement. Consequently, the first link could hardly strain even under high loads. Besides, another important observation is that, upon the onset of cracking, the rate of strain of the DE element is notably lower than that of the shear link, particularly in the critical elements of DE1 and SL2. It is therefore understood the significance of using prestress in the DE element in order to achieve high level of shear enhancements.

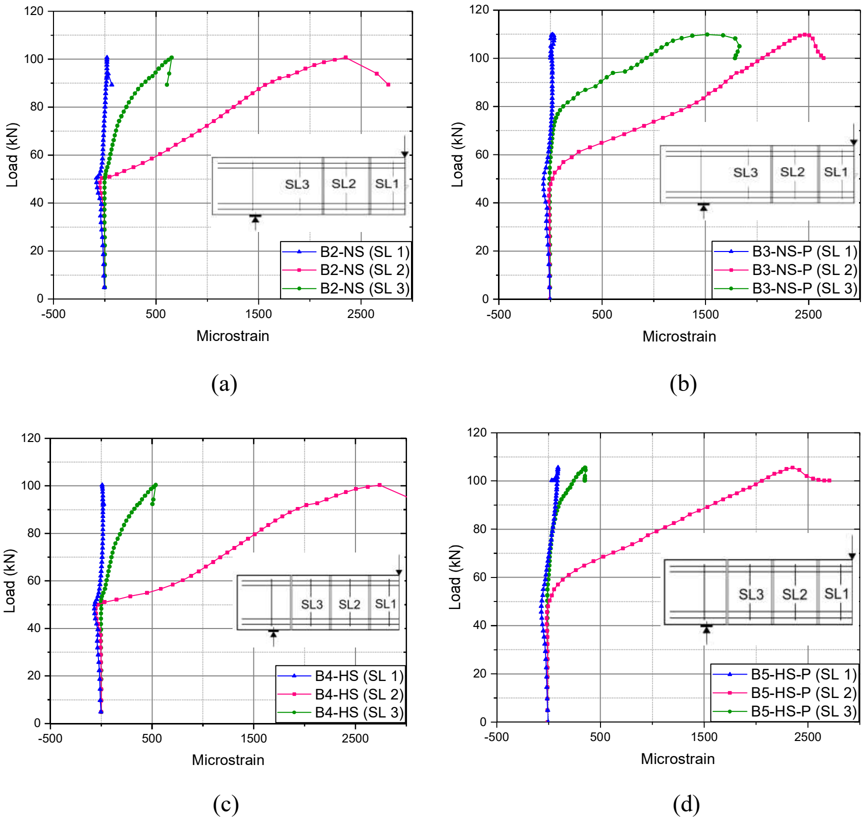

Fig. 7: Shear link strains: (a) B2-NS (b) B3-NS-P (c) B4-HS (d) B5-HS-P

4. Experimental study

An experimental study was executed in order to verify the potential of using prestress in DE shear retrofitting and to validate the numerical simulation findings. Five experimental beams those had similar properties to the beams in the numerical study were considered. Hence, the series included one control beam, two beams retrofitted in DE with normal steel reinforcement bars, and two beams retrofitted in DE with high-tensile steel reinforcement bars. The beam geometry and internal/DE reinforcement detailing is shown in **Fig. 2**. All the beams were subjected to 3-point bending and steel plates were used as bearings. Of note is that the same notation that was used for the beams in the numerical study is going be used for the experimental beams henceforth.

4.1. Material properties

Tensile tests were conducted for all the steel types and **Table 1** summarises the results. The concrete was designed for a target cube strength of 60 MPa and the mix proportions were: cement – 461 kg/m^3, water – 173 kg/m^3, fine aggregate – 750 kg/m^3, coarse aggregate (12.5 mm) – 1024 kg/m^3 and polycarboxylate superplasticizer – 3.2 l/m^3. Standard size cubes and cylinders were cast as control specimens. The cube testing revealed the compressive strengths of beams B1-C, B2-NS, B3-NS-P, B4-HS, B5-HS-P at the time testing were 66.1 MPa, 59.2 MPa, 59.2 MPa, 59.8 MPa and 59.8 MPa respectively. The static modulus, Poisson's ratio and the splitting tensile strength of the concrete of all the beams were 39.2 GPa, 0.19 and 3.6 MPa respectively.

4.2. DE retrofitting process

Holes of 15 mm and 10 mm diameter were drilled in order to install the H10 normal steel and 5 mm high-tensile steel DE reinforcements respectively. The hole surfaces were roughened by scraping the surface. Based on the recommendations of [6], a commercially available Hilti 500 epoxy was used as the bonding agent. According to the product specification, the characteristics of the epoxy were: 40 MPa tensile strength; 30-minute initial setting; and 5.5-hour hardening. The hole was first filled with epoxy resin and the DE bar was then inserted so that the epoxy resin fills up the holes thoroughly. For beams B3 and B5, the DE bars were prefabricated with threads at its ends and, upon the DE bars were embedded in the epoxy medium, the bottom of the bar was fixed to the beam using a nut. Subsequently, the top end of the DE bar was prestressed by tightening the screw against a steel stool that was placed on the beam surface, see **Fig. 8**. The prestress level was monitored through the strain gauge reading, and once the desired prestress level (40%) was achieved, the DE hole was topped up with epoxy through the stool. Before testing, the nut/stool arrangements were removed and the remaining bar sections were cut so that there was a flat beam surface.

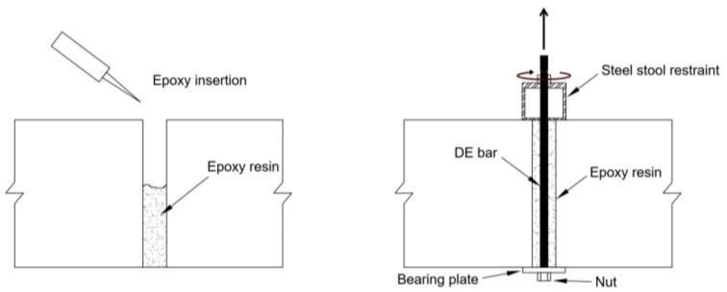

Fig. 8: Prestressing arrangement

4.3. Instrumentation

The beams were instrumented as shown in **Fig. 9(a)**. Here, the total load was read through a 50-ton capacity load cell and three linear resistance displacement transducers (LRDTs) were used (two at the supports and one at the mid-span) to estimate the mid-span deflection of the beam. Strain gauges were used to measure the strains in the DE bars and the shear links. All these instruments were connected to an automated data recording system. A 100-ton universal testing machine was used as the testing rig, see **Fig. 9(b).**

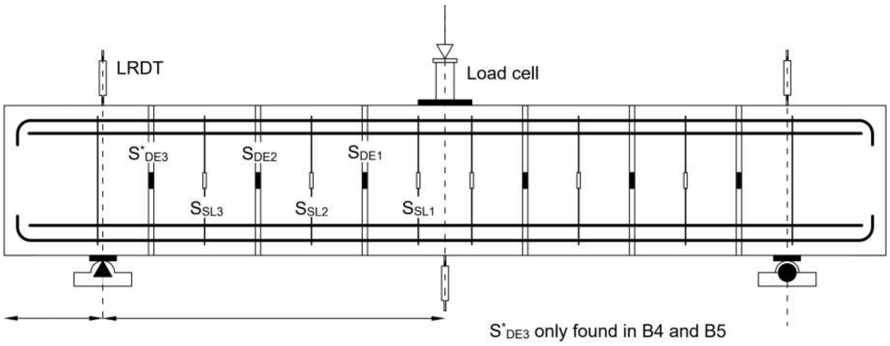

(a)

(b)

Fig.9: (a) Instrumentation; (b) Loading frame

4.4. Experimental results

All five beams failed in shear. **Table 4** summarises the failure loads and the pertaining shear enhancements. **Fig. 10** illustrates the load-displacement behaviours. The results highlight that the use of prestress in the DE system was able to achieve promising shear enhancements in contrast to the non-prestressed DE application. The level of extra shear enhancement achieved via the use of prestress was 25.8% and 18.7% at the normal steel and high-tensile steel scenarios respectively. It is of note that the compressive strength of the control specimen (B1-C) was higher than the retrofitted beams by about 7 MPa. If this particular discrepancy was taken into account across the failure load comparisons, the shear enhancement provided by the retrofitting system (and also by the prestressing) could have been even more highlighted.

Table 4

Experimental shear capacities

Specimen	Failure mode	Shear capacity (kN)	Shear enhancement (%)
B1-C	Shear	87.8	-
B2-NS	Shear	95.8	9.1
B3-NS-P	Shear	118.4	34.9
B4-HS	Shear	98.0	11.6
B5-HS-P	Shear	114.4	30.3

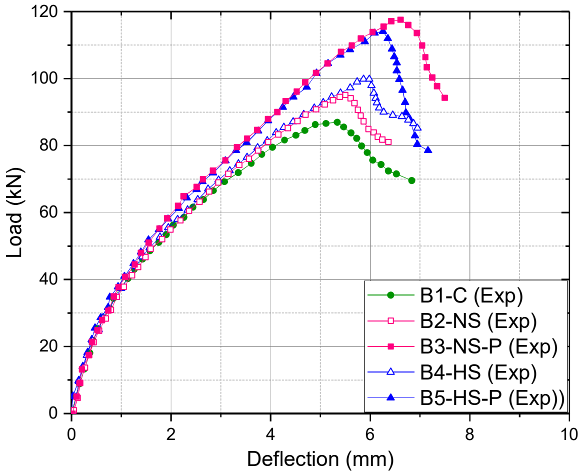

Fig.10: Experimental load-deflection behaviour

Overall, the experimental investigation highlighted that the use of prestress either in normal steel DE elements or in high-tensile steel DE elements was fairly useful to achieve extra shear enhancements where the former was observed to be slightly more promising. However, if the internal shear reinforcement was not of mild steel type, no such considerable shear gain could have been obtained with prestressing of normal steel DE bars.

5. Comparison of numerical predictions and experimental results

Both numerical and experimental studies highlighted the effectiveness of using prestress in the DE shear retrofitting system. Impressive improvements in terms of shear capacity and serviceability performance were observed with the use of prestress. In this light, further insights in the retrofitted behaviours are discussed in this section through comparisons of the two types of results. Of note is that the numerical models were updated so that to include the experimental concrete properties.

5.1 Shear capacity and load-displacement response

Table 5 compares the experimental shear capacities with the FE predictions. It highlights a good correlation between the two types of results where the mean and the standard deviation of the prediction accuracy are 98% and 5% respectively. The failure load of both non-prestressed DE strengthened beams were slightly over-predicted whereas that of the prestressed DE beams were under-predicted by about 8%. It is meanwhile of note that the shear enhancements (experimental) by the DE elements are 8.0 kN, 30.6 kN, 10.2 kN, and 26.6 kN respectively. If this supplement was predicted via TR55 [21] (which is the commonly used as an analytical tool for shear retrofitting) the predictions would be 19.3 kN, 22.2 kN, 5.8 kN, and 11.5 kN respectively. Hence, similarly to the conclusions in the literature, the inconsistency in the analytical predictions for the DE system was reiterated. Herein, the initial prestress was added to the strain recommended in TR55 for the retrofitting element to deal with the prestressed DE scenarios.

Table 5

Shear capacity comparisons

Specimen	Failure mode	FE shear capacity (kN)	Exp. shear capacity (kN)	FE/ Exp. ratio
B1-C	Shear	85.9	87.8	0.98
B2-NS	Shear	100.6	95.8	1.05
B3-NS-P	Shear	109.5	118.4	0.92
B4-HS	Shear	100.3	98.0	1.02
B5-HS-P	Shear	105.6	114.4	0.92

The load deflection responses of the beams are compared with the FE predictions in **Fig. 11**. It shows that the FE model precisely predicted the initial linear behaviour of the beams and reasonable correlations are observed over the non-linear behaviour as well. The non-linear stiffness of the retrofitted beams was slightly over-predicted, particularly for the non-prestressed DE scenarios.

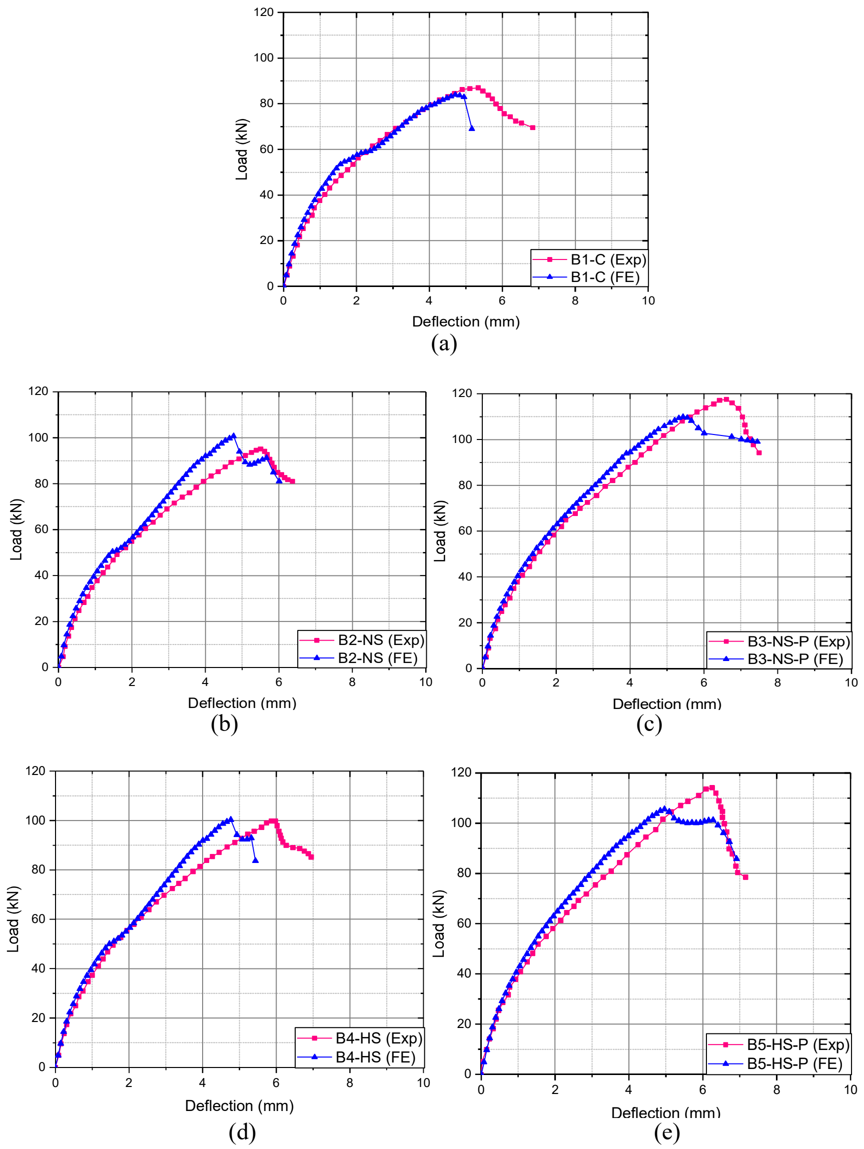

Fig 11: Experimental and numerical load-deflection comparisons; (a) B1-C; (b) B2-NS; (c) B3-NS-P; (d) B4-HS; (e) B5-HS-P

Based on the fact that the failure load of the beams with prestressed DE elements (in B3 and B5) were slightly under-predicted (by about 8%), apparently, the benefit of the prestress application was somewhat hindered in the FE model. Despite the DE bar in reality was a solid element, it was simulated as a truss element that went through nodes in the FE model. Consequently, it was deemed that the prestress might have not been appropriately distributed into the beam cross section in the simulations. Hence, as a potential modification, the DE element was simulated as a unit of four distinct truss elements those were through the corners of the (25 mm) concrete solid elements, see **Fig. 12**. As shown in **Fig. 13**, this particular modification was capable of increasing the prediction accuracy for the failure load of those two beams considerably, the pertaining prediction accuracy was then over 98%. Also, the predicted load-displacement response showed many similarities to that of the beams with non-prestressed DE elements. It was therefore deemed that more accurate FE predictions for the prestressed DE behaviour can be obtained by finer tuning of the FE mesh. Further explorations into it is identified as a matter for future work.

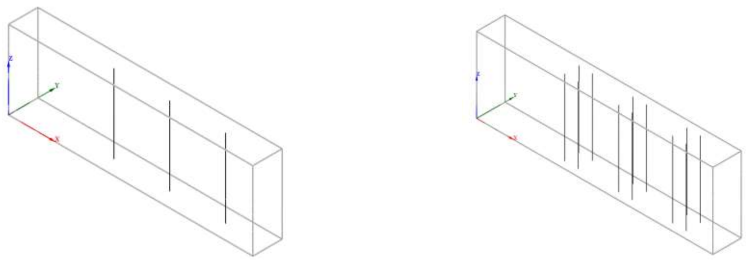

(a) (b)

Fig 12: DE element simulation; (a) as a single truss element; (b) as four-unit truss elements

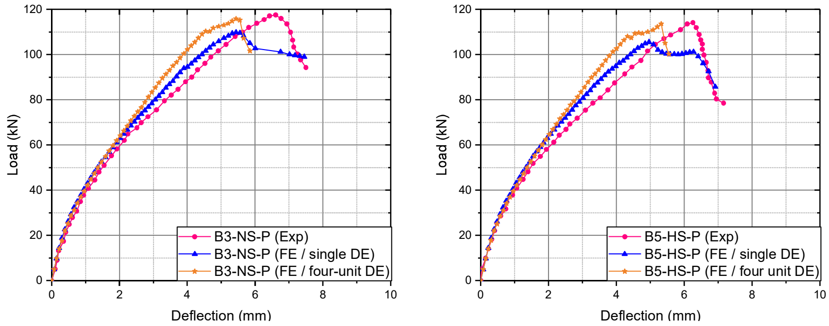

(a) (b)

Fig.13: Load-displacement comparison at modified DE element simulation: (a) B3-NS-P; (b) B5-HS-P

5.2. Crack patterns

A comparison of FEM predicted crack patterns with the experimental results was made as shown in **Fig. 14**. It is observed that the predictions on crack locations, extent, orientations show appreciable correlations with the experimental results. As should be theoretically expected, the crack angle steepened with the use of prestress in the DE elements, and that behaviour was also well captured by the FE modelling.

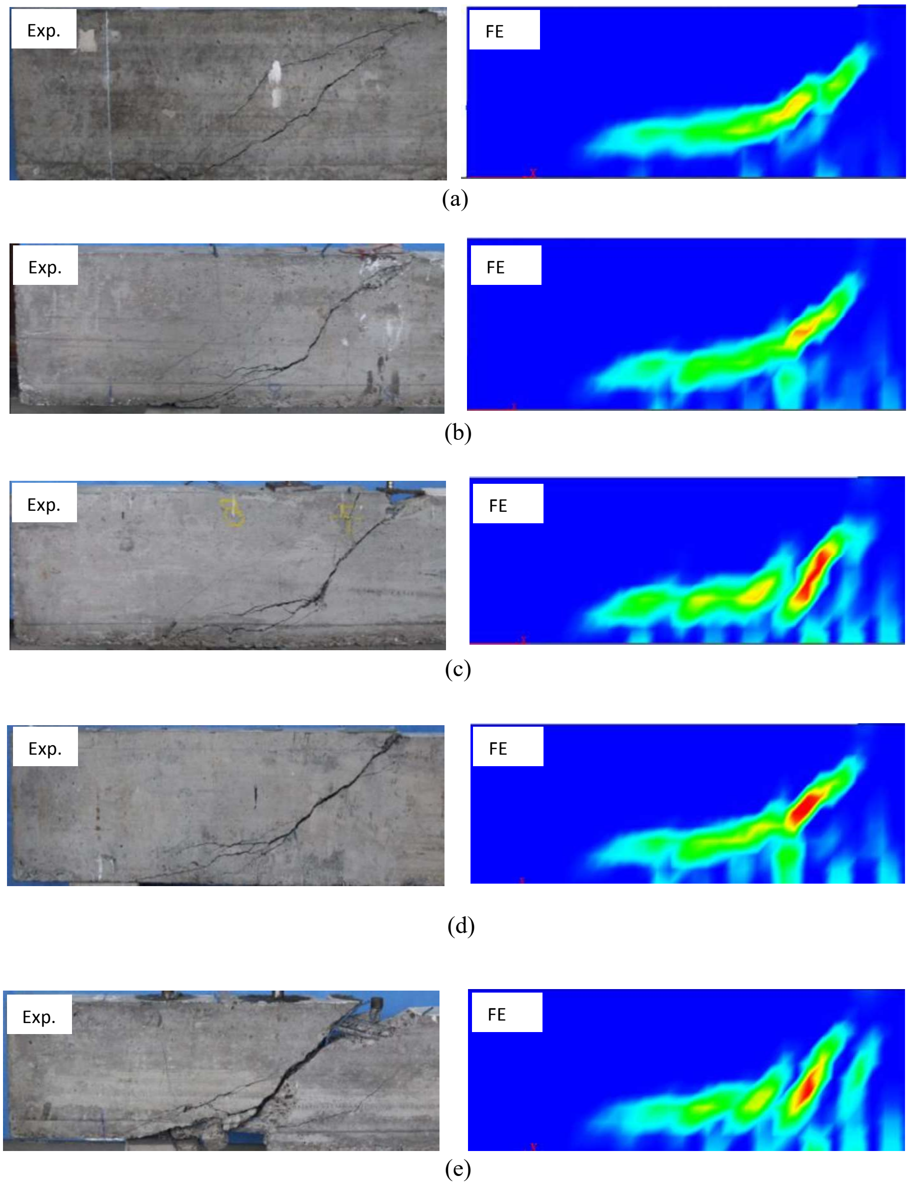

Fig 14: Crack pattern comparisons; (a) B1-C; (b) B2-NS; (c) B3-NS-P; (d) B4-HS; (e) B5-HS-P

It is meanwhile of note that, even though the FE simulations predict the cracking to be symmetric over the both shear spans, practically one shear span is subjected to dominant cracking in contrast to the other. This is mainly because of the heterogeneity of concrete and of the non-ideal experimental conditions. In fact all the comparisons in Fig.14 were limited to the cracking in the critical shear span. The literature shows examples of modifying the FE mesh in order to obtain unsymmetrical cracking from FE simulations. Blomfors et al. [38] studied FE simulation of pre-cracked RC beams and showed that good correlation in cracking and in load prediction could be obtained via weakening of the concrete elements (in the FE mesh) along the pre-crack locations. Accordingly, a preliminary attempt was made in this study to weaken the FE mesh deliberately along the major crack path (observed experimentally) in the critical shear span with the intention of obtaining asymmetric cracking. **Fig. 15** shows this application into the full FE model of B5-HS-P (this beam was selected for this discussion because it had a dominant shear crack). Based on the information in [38], herein the weakened concrete elements were assigned with 25% of the original tensile strength and with zero Poisson's ratio.

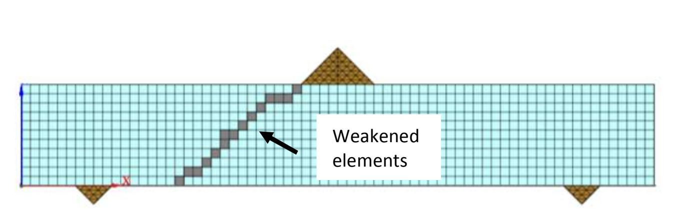

Fig. 15: Introduction of weak concrete elements to Fe model of B5-HS-P

Fig. 16 compares the experimental crack pattern with that in the modified FE model output for B5-HS-P. As expected, the correlation between the full beam experimental cracking and the FE simulation was improved. However, the failure load prediction was reduced by about 5% (it was originally an under-prediction) . Similar trend was observed also for the other beams, the reduction in prediction was sometimes as high as 11%. Hence, even though the crack comparison was improved through this particular FE modification, the load capacity prediction was compromised. It was therefore deemed that the considered modification, which was proven to be effective for pre-cracked structures, needs further exploration before its utilisation on simulating asymmetric behaviour of RC beams during 3-point bending. This is identified as an essential matter for future work.

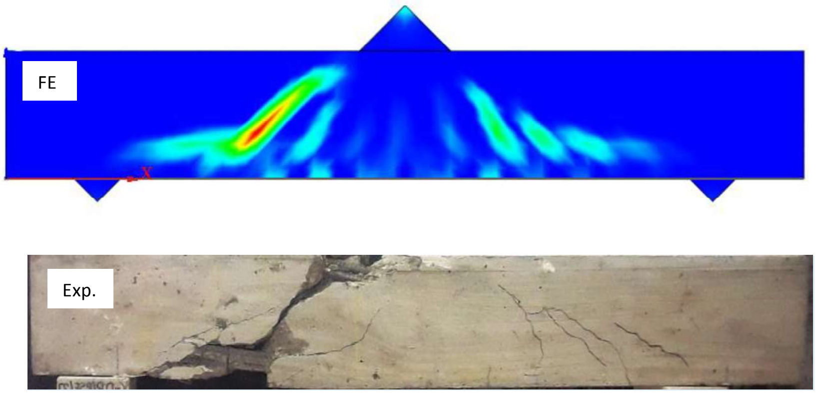

Fig. 16: Crack pattern comparison with full model for B5-HS-P

Commented [HD1]: Reviewer 3, comment 1

5.3. DE reinforcement strains

In order to see the prediction accuracy for the local beam behaviour further, the strain in the DE bar of the retrofitted experimental beams was compared with the FE model predictions, see **Fig. 17**. The DE element that was next to the load point (DE1) was selected for this comparison as it was identified to be critical previously. Since a strain gauge reading reflects an average strain level for a short length (i.e., not of a spot measurement), the average strain of three elements of the DE mesh (i.e., of 75 mm length) at the middle of the bar was selected for the comparison.

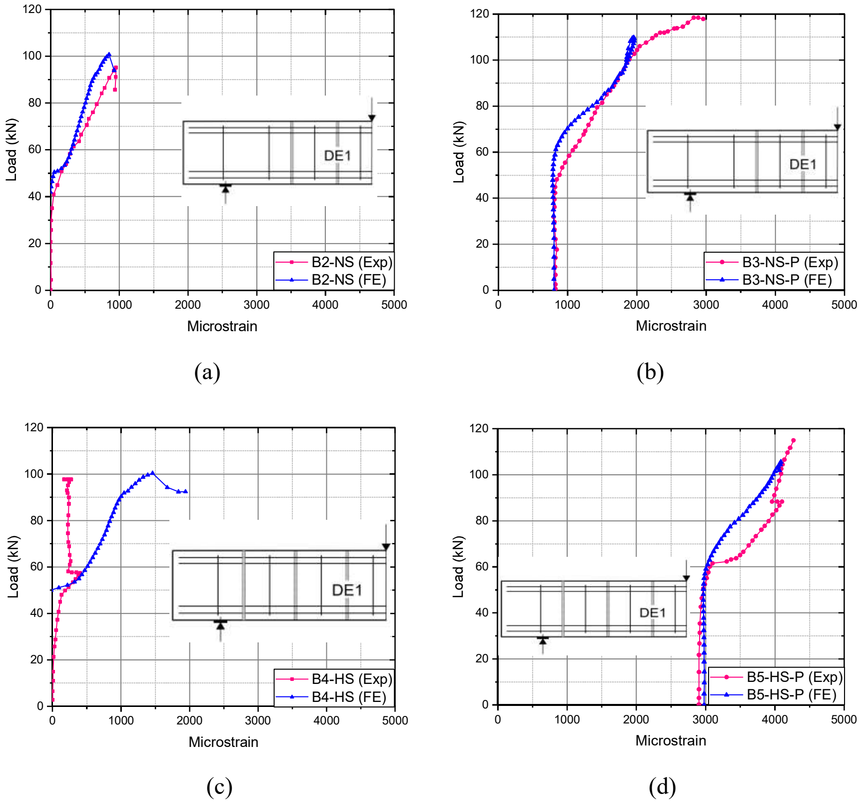

Fig 17: DE bar strain relations for specimens; (a) B2-NS; (b) B3-NS-P; (c) B4-HS; (d) B5-HS-P

Fig. 17 shows that the passive nature of the DE element (over the un-cracked behaviour) and the subsequent straining behaviour of the DE element in all the beams were predicted reasonably accurately by the FE model. Of note is that the strain gauge in B4-HS failed with the onset of staining. This comparison particularly highlights the potential of the non-linear modelling to deal with prestressed DE elements.

6. Parametric analysis

In the light of non-linear simulation potential of the prestressed DE system behaviour is thus proved in this study, parametric numerical studies can be used to identify optimum retrofitting configurations for the prestressed system. Accordingly, a brief parametric investigation was carried out to assess the sensitivity of parameters of: prestress level; DE bar size; and DE bar location (relative to the internal shear reinforcement, on the shear response of prestressed DE retrofitted system. Specimen B3-NS-P is chosen for this purpose of study since it represented the most effective system. **Fig.18** summarizes the results.

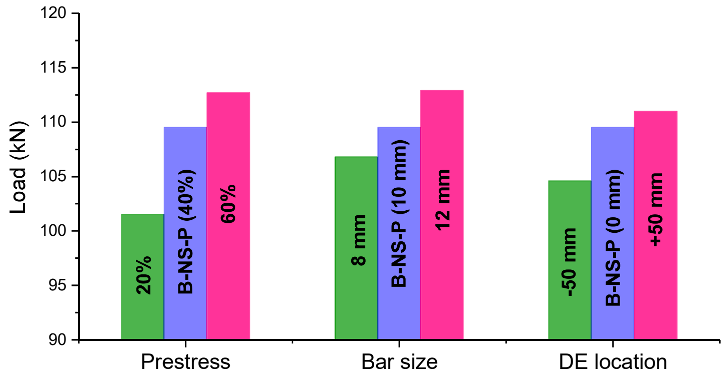

Fig.18: Parametric analysis results

As illustrated in **Fig.18**, increment of prestress from 20% to 60% shows increase of the retrofitted shear capacity where the improvement at the first increment (20% to 40%) is significant than that in the second increment. The internal shear link governed the failure of all three cases. Similarly, the shear capacity increases with the increasing bar diameter increases. where again the internal shear link capacity dictated the beam strength. It is thus highlighted that the shear gain cannot only be improved via stronger retrofitting system. Meanwhile, the parametric analysis shows that the optimum DE location could be different from the middle point between the internal shear links. Here, when the DE bar was shifted 50 mm towards the loading point, the effectiveness of the system is increased. In fact, when the moment-shear interaction in the beam region is considered [37], condensation of shear reinforcement towards the loading point of a 4-point bending scenario can be expectable. The parametric study thus highlights numerous parametric sensitivities that could exist in the prestressed DE shear strengthening systems. A comprehensive study into is identified as a matter for future work.

7. Conclusions

This study explored the effectiveness of using prestress in the deep embedded (DE) system for shear retrofitting of RC beams via non-linear numerical simulations and an experimental study. Two scenarios of using normal steel and high-tensile steel DE bars were considered. The following conclusions can be drawn based on the findings.

a) The non-linear numerical simulations showed that the use of prestress in the DE shear retrofitting system was impressive. The application of 40% prestress to the normal and high-tensile reinforcement bars resulted in 31% and 26.3% shear enhancements respectively where that was about 20% when those bars were not prestressed. The numerical results also showed that the critical area of the beam to be retrofitted was the vicinity of the load point.

b) The experimental study confirmed the main finding of the numerical study that the prestressing of DE bars was capable of providing extra shear strength to the RC beams. Here, the use of 40% prestress resulted in 34.9% and 30.3% shear enhancements for the beams with normal and high-tensile reinforcement DE bars respectively. In contrast, the shear enhancements were 9.1% and 11.6% respectively when the bars were not prestressed.

c) The use of prestress in normal steel DE elements was observed to be slightly more effective than using prestress in the high-tensile DE elements. However, if the internal shear reinforcement was not of mild steel type, no such favourability could have been obtained with prestressing of normal steel DE bars.

d) The experimental results verified the numerical predictions for the global and local behaviours of the beams. Good correlations between the two types of results in terms of load-displacement behaviour, DE reinforcement strains and crack patterns were observed. The shear strength gain owing to the use of prestress was slightly under-predicted by the non-linear numerical model and it was also identified that the numerical model can further be tuned up.

e) The ultimate strain levels of the DE elements were considerably higher in the prestressed beams than the other beams. Hence, the strength in the DE elements were utilised efficiently with the application of prestress. Meanwhile, the beams with prestressed DE elements exhibited steeper crack angles in contrast to the other beams, and hence, the concrete contribution was noted to be improved owing to the prestress. Also, the undesirable straining of the internal shear reinforcement was hindered as a consequence of the prestress usage.

f) Both numerical and experimental findings highlighted that the use of prestress in the DE system improved the post-cracking stiffness of the beam and controlled crack propagation in the shear span. Hence, the prestress application enhanced the serviceability performance of the beams as well.

g) The parametric analysis highlighted the sensitivity of the major parameters towards the performance of the prestressed DE system. Conduction of comprehensive such analysis is important to identify optimum retrofitting configurations for the prestressed DE shear retrofitting system and it is identified as a matter for future work. In addition, experimental investigation of the potential of using prestress in FRP DE systems is also recommended.

Acknowledgements

NRC 17-047 grant provided financial support for the project. The assistance provided by Wilfred Benaja and the technical staff of the Materials laboratory of the University of Peradeniya is highly appreciated.

References

[1] Lees, J.M., Winistörfer, A.U. and Meier, U., 2002. External prestressed carbon fiber-reinforced polymer straps for shear enhancement of concrete. *Journal of Composites for Construction*, *6*(4), pp.249-256.

[2] Kesse, G. and Lees, J.M., 2007. Experimental behaviour of reinforced concrete beams strengthened with prestressed CFRP shear straps. *Journal of Composites for Construction*, *11*(4), pp.375-383.

[3] Dirar, S., Lees, J.M. and Morley, C., 2013. Phased nonlinear finite-element analysis of precracked RC T-beams repaired in shear with CFRP sheets. *Journal of Composites for Construction*, *17*(4), pp.476-487.

[4] Kurukulasuriya, M.C., Rathnayake, H.S. and Yapa, H.D., 2017, Optimum Shear Strengthening of Reinforced Concrete Beams using an Un-bonded CFRP Strap Shear Retrofitting System, Proceedings of the 8th International Conference on Advanced Composites in Construction, pp.107-112.

[5] Valerio, P. and Ibell, T.J., 2003. Shear strengthening of existing concrete bridges. *Proceedings of the Institution of Civil Engineers-Structures and Buildings*, *156*(1), pp.75-84.

[6] Valerio, P., Ibell, T.J. and Darby, A.P., 2009. Deep embedment of FRP for concrete shear strengthening. *Proceedings of the Institution of Civil Engineers-Structures and Buildings*, *162*(5), pp.311-321.

[7] Bousselham, A. and Chaallal, O., 2008. Mechanisms of shear resistance of concrete beams strengthened in shear with externally bonded FRP. *Journal of Composites for Construction*, *12*(5), pp.499-512.

[8] Hoult, N.A. and Lees, J.M., 2009. Efficient CFRP strap configurations for the shear strengthening of reinforced concrete T-beams. *Journal of Composites for Construction*, *13*(1), pp.45-52.

[9] Mofidi, A. and Chaallal, O., 2011. Shear strengthening of RC beams with externally bonded FRP composites: Effect of strip-width-to-strip-spacing ratio. *Journal of Composites for Construction*, *15*(5), pp.732-742.

[10] Chaallal, O., Mofidi, A., Benmokrane, B. and Neale, K., 2011. Embedded through-section FRP rod method for shear strengthening of RC beams: Performance and comparison with existing techniques. *Journal of composites for construction*, *15*(3), pp.374-383.

[11] Godat, A., L'hady, A., Chaallal, O. and Neale, K.W., 2012. Bond behavior of the ETS FRP bar shear-strengthening method. *Journal of Composites for Construction*, *16*(5), pp.529-539.

[12] Godat, A., Labossière, P., Neale, K.W. and Chaallal, O., 2012. Behavior of RC members strengthened in shear with EB FRP: Assessment of models and FE simulation approaches. *Computers & structures*, *92*, pp.269-282.

[13] De Lorenzis, L. and Nanni, A., 2001. Shear strengthening of reinforced concrete beams with near-surface mounted fiber-reinforced polymer rods. *Structural Journal*, *98*(1), pp.60-68.

[14] Moradi, E., Naderpour, H. and Kheyroddin, A., 2020. An experimental approach for shear strengthening of RC beams using a proposed technique by embedded through-section FRP sheets. *Composite Structures*, *238*, p.111988.

[15] Yapa, H.D. and Lees, J.M., 2014 (a). Rectangular reinforced concrete beams strengthened with CFRP straps. *Journal of Composites for Construction*, *18*(1), p.04013032.

[16] Yapa, H.D. and Lees, J.M., 2014 (b). Optimisation of shear strengthened reinforced concrete beams. *Proceedings of the Institution of Civil Engineers-Engineering and Computational Mechanics*, *167*(2), pp.82-96.

[17] Caro, M., Dirar, S., Quinn, A. and Yapa, H., 2021. Shear strengthening of existing reinforced concrete beams with embedded bars–an overview. *Proceedings of the Institution of Civil Engineers-Structures and Buildings*, pp.1-14.

[18] Raicic, V., Ibell, T., Darby, A., Evernden, M. and Orr, J., 2017, January. Effectiveness of the Deep Embedment (DE) Technique for Shear Strengthening of Reinforced Concrete Continuous T-beams. In *Advanced Composites in Construction, ACIC 2017-*

Proceedings of the 8th Biennial Conference on Advanced Composites in Construction, pp. 120-125.

[19] Barros, J.A. and Dalfré, G.M., 2013. Assessment of the Effectiveness of the Embedded Through- Section Technique for the Shear Strengthening of Reinforced Concrete Beams. *Strain*, *49*(1), pp.75-93.

[20] Qapo, M., Dirar, S. and Jemaa, Y., 2016. Finite element parametric study of reinforced concrete beams shear-strengthened with embedded FRP bars. *Composite Structures*, *149*, pp.93-105.

[21] The Concrete Society, 2012. *Technical report TR55: Design guidance for strengthening concrete structures using fibre composite materials*. Camberley.

[22] Mofidi, A., Chaallal, O., Benmokrane, B. and Neale, K., 2012. Experimental tests and design model for RC beams strengthened in shear using the embedded through-section FRP method. *Journal of Composites for Construction*, *16*(5), pp.540-550.

[23] Breveglieri, M., Aprile, A. and Barros, J.A., 2014. Shear strengthening of reinforced concrete beams strengthened using embedded through section steel bars. *Engineering Structures*, *81*, pp.76-87.

[24] Sogut, K., Dirar, S., Theofanous, M., Faramarzi, A. and Nayak, A.N., 2021. Effect of transverse and longitudinal reinforcement ratios on the behaviour of RC T-beams shear-strengthened with embedded FRP bars. *Composite Structures*, 113622, pp.1-12.

[25] Dirar, S. and Theofanous, M., 2017, Large-scale Reinforced Concrete T-beams Strengthened in Shear with Embedded GFRP Bars, *Advanced composites in construction*, pp. 114-119

[26] Yapa, H.D., Fatheen, M. and Ahamed, S., 2019, Efficient Shear Retrofitting of Reinforced Concrete (RC) Beams using Prestressed Deep Embedded (DE) FRP Bars, Proceedings of the 9th *Advanced Composites in Construction*, pp. 17 – 22.

[27] Yang, Y., Feng, S., Xue, Y., Yu, Y., Wang, H. and Chen, Y., 2019. Experimental study on shear behavior of fire-damaged reinforced concrete T-beams retrofitted with prestressed steel straps. *Construction and Building Materials*, *209*, pp.644-654.

[28] MIDAS FEA V 2.8, 2008. Nonlinear and Detail FE Analysis System for Civil Structures, FEA Analysis and Algorithm Manual (2008)

[29] Rots, J.G. and Blaauwendraad, J., 1989. Crack models for concrete, discrete or smeared? Fixed, multi-directional or rotating?. *HERON, 34 (1), 1989*.

[30] Godat, A., Chaallal, O. and Neale, K.W., 2013. Nonlinear finite element models for the embedded through-section FRP shear-strengthening method. *Computers & Structures*, *119*, pp.12-22.

[31] Vecchio, F.J. and Collins, M.P., 1993. Compression response of cracked reinforced concrete. *Journal of structural engineering*, 119(12), pp.3590-3610.

[32] Selby, R.G. and Vecchio, F.J., 1997. A constitutive model for analysis of reinforced concrete solids. *Canadian journal of civil engineering*, 24(3), pp.460-470.

[33] Feenstra, P.H., De Borst, R. and Rots, J.G., 1991. A comparison of different crack models applied to plain and reinforced concrete. *Proceedings of the International RILEM/ESIS Conference Fracture Processes in Concrete, Rock and Ceramics*, pp. 629-638

[34] Eligehausen, R., Bertero, V.V. and Popov, E.P., 1983. Local bond stress-slip relationships of deformed bars under generalized excitations: Tests and analytical model. *Earthquake Engineering Research Center, Univ. of California, Berkeley, Calif., Report No. EERC*, pp.83-23.

[35] Cosenza, E., Manfredi, G. and Realfonzo, R., 1997. Behavior and modeling of bond of FRP rebars to concrete. *Journal of composites for construction*, 1(2), pp.40-51.

[36] Comité Euro-International du Béton, C.E.I., 2010. *CEB-FIP model code 2010.* Willey

[37] Vecchio, F.J., and Collins, M.P., 1986. The modified compression-field theory for reinforced concrete elements subjected to shear. *ACI J.*, *83*(2), pp.219-231.

[38] Blomfors, M., Berrocal, C.G., Lundgren, K. and Zandi, K., 2021. Incorporation of pre-existing cracks in finite element analyses of reinforced concrete beams without transverse reinforcement, Engineering Structures, 221, pp. 1-14

Commented [HD2]: Reviewer 3, comment 1